



Nonlinear behavior of the current–voltage characteristics for erbium-doped PVA polymeric composite films

H. I. Elsaedy¹ · H. Elhosiny Ali^{1,2} · H. Algarni¹ · I. S. Yahia^{1,3}

Received: 18 September 2018 / Accepted: 27 December 2018 / Published online: 7 January 2019
© Springer-Verlag GmbH Germany, part of Springer Nature 2019

Abstract

The universal casting method for an aqueous solution has been used to synthesize PVA solid samples with 0, 0.037, 0.37, 3.7, 18.5, and 37 wt% of Er³⁺-ions. The semi-crystalline nature of solid films was proved by analyzing the pattern of the XRD, while the complex formation has been confirmed via FTIR spectroscopy. SEM shows the formation of clusters of the Er³⁺-ions on the superficiality of PVA. The optical parameters, dielectric permittivity, and *I*–*V* characteristics have been studied. The incident light is completely absorbed in UV-region by PVA: 37 wt% Er³⁺-sample. Moreover, the indirect energy, E_{g1} , gap decreased from 4.98 to 4.74 eV, whereas the index of refraction increased from 1.53 to 2.85 with Er³⁺-ions concentration. Dielectric permittivity decreases with a high proportion of Er³⁺-ions in PVA and an interesting nonlinear behavior of *I*–*V* characteristics is observed in PVA: 37 wt% Er³⁺-sample. The characteristics of synthesized materials revealed that it can be used for manufacturing cheaper varistor device, UV-protector, and optoelectronic applications.

1 Introduction

A prototype polyvinyl alcohol, PVA, has special recognition from scientists due to its wide and promising usages in manufacturing devices, as optoelectronics, micro-optics, varistors, sensors, etc. [1–3]. The optical properties and electrical conduction mechanism in polymeric materials vary according to the contents' level and the type of the fillers [4–6]. It is well known that the electronic conductivity of the polymer is caused by the carrier mobility that appears in the electronic system via positive or negative particles [7, 8]. The conductivity of polymeric films can be modified by filler doping grade and type [4, 9], as it depends on the transition of electrons between various chains.

In recent time, the rare earth, RE, salts are attracting a considerable attention in composites because of their promotional properties [10, 11]. The aptitude to increase the light output and also, to reduce reflection loss has a great application in nonlinear optics, optical information storage, optical fiber, light-emitting diodes, lasers and optical switching [12]. Moreover, it is more vital when it has been utilized for doping ceramic resistor devices [13]. It was reported before that RE salts with polymer form a hydroxide complexes by the help of weak bond [14]. So, when RE-ions are doped in pure material, they produce significant properties [5].

Owing to such tremendous modifications in the key properties of PVA through RE ions, it seems to be justified to work further using a novel RE element for enhancing the properties of the parent polymer matrix. Thus, in current work, we aimed to investigate the effect of erbium nitrate with various weight proportions on crystallinity and dielectric of all as-prepared samples. Moreover, the optical functional parameters will also be calculated from transmission and absorption spectra. Also, the ability to use the synthesized materials in varistor–polymer applications was investigated by measuring *I*–*V* characteristics.

✉ H. Elhosiny Ali
hibrahim@kku.edu.sa; hithamph@gmail.com;
hitham_ph@zu.edu.eg

¹ Advanced Functional Materials and Optoelectronic Laboratory (AFMOL), Department of Physics, Faculty of Science, King Khalid University, P.O. Box 9004, Abha, Saudi Arabia
² Physics Department, Faculty of Science, Zagazig University, Zagazig 44519, Egypt
³ Nanoscience Laboratory for Environmental and Bio-medical Applications (NLEBA), Semiconductor Lab, Physics Department, Faculty of Education, Ain Shams University, Roxy, Cairo, Egypt

2 Experimental details

A 0.001, 0.01, 0.1, 0.5, and 1 g of erbium (III) nitrate ($\text{Er}(\text{NO}_3)_3 \cdot 6\text{H}_2\text{O}$), with 4 N purity, was added to 4 N purity of polyvinyl alcohol (PVA). PVA was diluted in distilled water to cast the proposed samples which are hereafter called as pure PVA (PVA: 0 wt% Er^{3+}), PVA: 0.037 wt% Er^{3+} , PVA: 0.37 wt% Er^{3+} , PVA: 3.7 wt% Er^{3+} , PVA: 18.5 wt% Er^{3+} and PVA: 37 wt% Er^{3+} , respectively. The percentage of Er^{3+} weight in PVA was calculated by

$$W(\%) = \frac{W_{\text{Er}} \times 100}{W_{\text{PVA}} + W_{\text{Er}}}, \quad (1)$$

where W_{Er} and W_{PVA} refer to ($\text{Er}(\text{NO}_3)_3 \cdot 6\text{H}_2\text{O}$) and PVA weights, respectively. The mixtures of PVA with different weights of Erbium Nitrate were agitated, for a homogeneous solution, in ultrasonic during 2 min. After that, they were poured into an equal-sized flat petri-dishes. For solid films, the mixtures were dried by adjusting the oven to 40 °C for 4 days. Colorless and flexible composite films with a homogeneous average thickness equal to ~0.1 mm.

The crystalline structure of the samples was measured via XRD-6000 diffractometer (Shimadzu model). The XRD with wavelength $\lambda = 1.5418 \text{ \AA}$, of a monochromatic source ($\text{CuK}\alpha$), was used to measure the phases of Er^{3+} -ions doped PVA samples between 5° and 60° range with angular rate of 0.02/s.

Moreover, the influence of Er^{3+} -ions content on the functional groups of PVA was studied by measuring the transmission spectra in 400–4000 cm^{-1} wavenumber range via FTIR spectrometer (Thermo Nicolet 6700).

The morphology of the samples and the size of Er^{3+} -ions in the doped PVA films were measured with the help of Scanning Electron Microscopy (model: JSM-6360).

The JASCO V-570 spectrophotometer was used for monitoring the transmittance, T and absorbance, B , spectra of the samples between 190 and 2500 nm range.

Furthermore, a sinusoidal voltage with frequencies between 3 kHz and 10 MHz range was applied on the samples, via a KEITHLEY characterization system (4200-SCS), for testing the dielectric capacitance, dielectric loss and I - V characteristic curve of all as-prepared Er^{3+} -ions doped PVA films. For these measurements, a sample holder with brass electrodes was used.

3 Results and discussion

3.1 X-ray diffraction analysis

The diffraction peaks of Er^{3+} /PVA samples with different concentrations (0, 0.037, 0.37, 3.7, 18.5 and 37 wt%) are detected via the XRD. The hard-sharp signal at ~19.54° is absent in all PVA samples (Fig. 1). This confirms the crystal structure of PVA closest to amorphous nature which agrees well with the previous work [2, 15]. The figure also shows that the width of this peak increases and thus the crystallinity decreases with further increase of Er^{3+} -content. So, the crystallinity degree strongly depends on how much bonds formed between the Er^{3+} -ion and the hydrogen in the backbone of PVA [16]. The significant decrease in the relative intensity of the sample peaks can be related to the high concentration of Er^{3+} -ion as it is clear in PVA: 18.5 wt% Er^{3+} and PVA: 37 wt% Er^{3+} -films. For calculating the induced strain and the mean crystallite size, the following relations are employed [17, 18]:

$$D = \frac{k\lambda}{\beta \cos \theta}, \quad (2)$$

$$\varepsilon = \frac{\beta}{4 \tan \theta}, \quad (3)$$

where ε , D (nm) and β are denoted, respectively, to strain, crystal size and FWHM. By taking $k = 0.9$, the nano-metric of the mean size of crystallites decreased with erbium ion increment in the polymer sample, as illustrated in Table 1. This means that the preparation technique allows the complex formation of the PVA with Er^{3+} -ions. However, it is

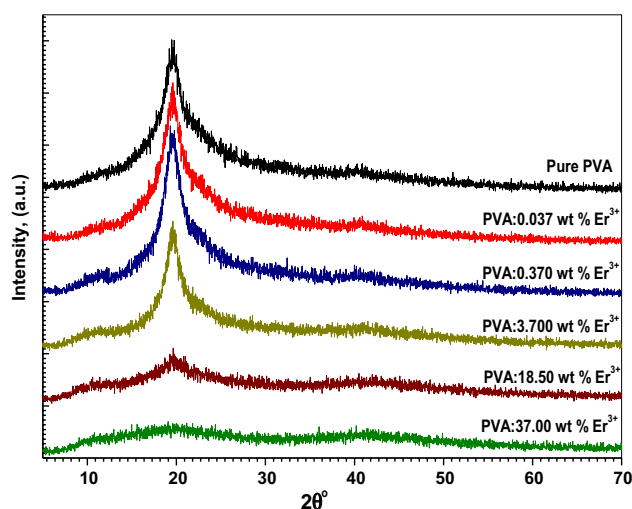
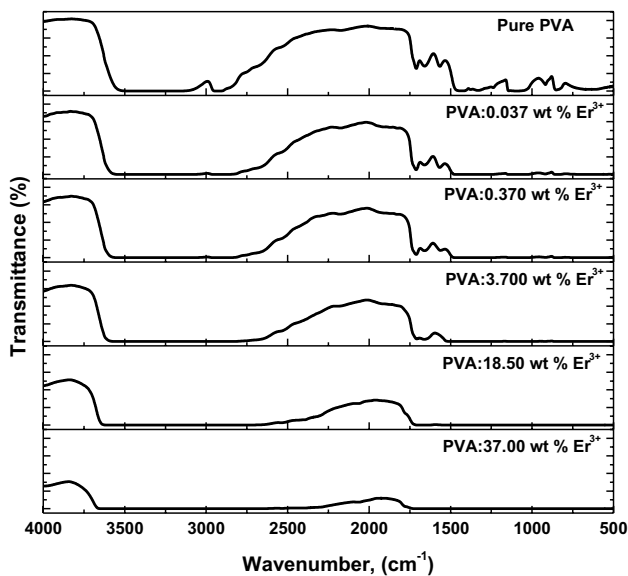


Fig. 1 X-ray diffraction (XRD) patterns of pure PVA and various wt% Er^{3+} -doped PVA polymeric samples

Table 1 Crystal size, internal induced strain, optical dispersion constants, direct and indirect energy band gap for different wt% erbium nitrate–PVA polymeric composite samples

Er ³⁺ /PVA	0 wt%	0.037 wt%	0.37 wt%	3.7 wt%	18.5 wt%	37 wt%
2θ	19.5443	19.5516	19.5433	19.595	19.750	23.890
D (nm)	3.2900	4.1300	4.1100	4.0600	3.2300	3.1100
ϵ	0.0618	0.0493	0.0495	0.0502	0.0628	0.0653
E_{g1} (eV)	4.9810	4.9530	4.9180	4.8290	4.7920	4.7390
E_{g2} (eV)	–	–	–	3.0140	3.5170	3.6240
E'_g (eV)	5.6010	5.5370	5.4630	5.2620	5.1960	5.0780
E''_g (eV)	–	–	–	–	–	4.0570
E_d (eV)	8.1300	1.3700	3.5700	7.8000	6.8700	11.770
E_s (eV)	6.3200	3.7000	2.9200	2.5300	2.4700	2.2100

**Fig. 2** FTIR spectra of pure PVA and different wt% Er³⁺-doped PVA polymeric samples

also observed that the internal induced strain increased with more addition of Er³⁺-ion contents, which is explained by the increment of the distortion in the base sample.

3.2 The functional groups of Er³⁺-doped PVA films characterized using FTIR spectroscopy

FTIR analysis was performed to examine the influence of the Er³⁺-ions on the PVA matrix at the molecular level. Figure 2(a–f) display the FTIR spectra of all samples. The strong main band between 3492 and 3146 cm⁻¹ is corresponding to stretching vibration of O–H in the pure PVA sample as illustrated in Fig. 2a. Moreover, the absorption band at 2942 cm⁻¹ is assigned to –CH₂ asymmetric stretching vibration, whereas the other bands observed at 1709 cm⁻¹ and 1094 cm⁻¹ are attributed to the stretching mode of C=O and C–O–C groups. The absorption bands that exist at 1565 cm⁻¹, 1422 cm⁻¹, 1375 cm⁻¹, and 851 cm⁻¹

arised due to –OH and –CH bending, C–H wagging, as well as the out-of-plane C–H vibrations, respectively [19, 20].

As presented in Fig. 2(b–f), there is a shift in the peaks of Er³⁺-ion doped PVA samples. The hydroxyl functional band is shifted with further Er³⁺-ion content to 3172–3017, 3620–2710, and 3648–2652 cm⁻¹ for PVA: 3.7 wt% Er³⁺, PVA: 18.5 wt% Er³⁺, and PVA: 18.5 wt% Er³⁺-samples, respectively, due to the chemical conjugation of Er³⁺-ion with PVA molecules. Moreover, the functional group's intensity decreased with more charge escorted by the increment of Er³⁺-ions' content in the PVA matrix. The shift and the decrease in the intensity of the peaks indicate the augmentation of the crystalline degradation within Er³⁺-doped PVA polymeric samples, which is in correlation with XRD results and also was reported in the literature for polymeric composite films [21].

3.3 Microstructure surface morphology of Er³⁺-doped PVA films by SEM

Figure 3(a–c) show the morphology surfaces of the sample before and after embedding Er³⁺-ions by means of SEM. The gray color refers to the host PVA, while the whitish one depicts Er³⁺-ions in the matrix. It is observed that at the low concentration of 0.37 wt% Er³⁺-ions, the particles are spherical and homogeneously distributed over the entire surface, while the particles agglomerated with further increase of doping content level and form a cluster with different distribution as shown in Fig. 3c. These results are similar to the previous work reported on La³⁺-doped PVA and PVA–Al₂O₃ composite films [2, 22].

3.4 The optical analysis of Er³⁺/PVA composite films

The optical UV–Vis–NIR transmission spectra of pure and Er³⁺-ions-doped PVA samples are displayed as seen in Fig. 4. It is clear from this figure that the transmittance values, in the visible spectrum, are about 90% of the base sample and decreases gradually to ≈ 84% with Er³⁺-ions ratio in the core matrix. In a similar manner, the results are also

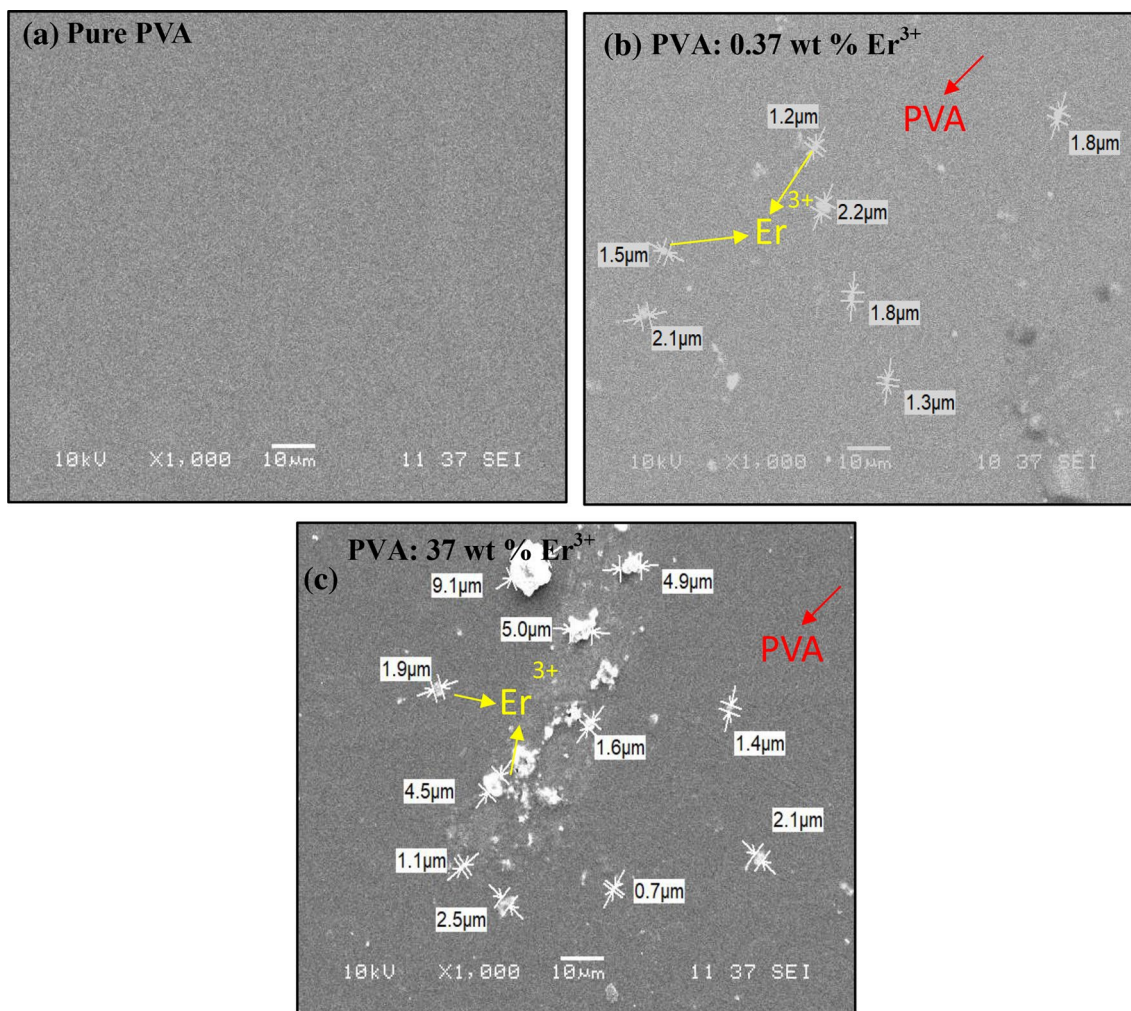


Fig. 3 SEM images of pure PVA (a), PVA:0.37 wt% Er³⁺ (b), and PVA: 37 wt% of Er³⁺-samples (c)

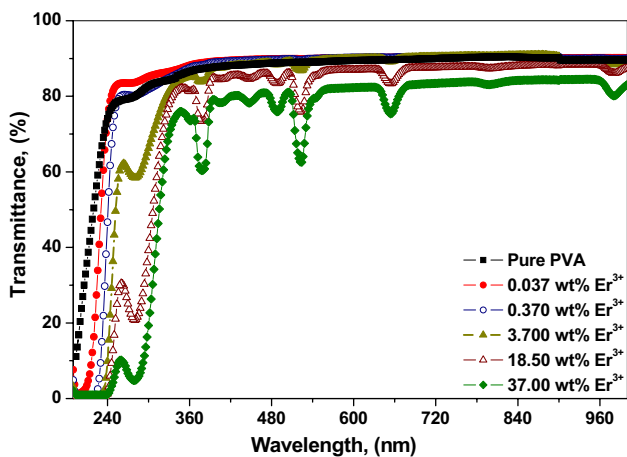


Fig. 4 UV-vis-NIR transmittance of pure PVA and various wt% Er³⁺-doped PVA polymeric samples

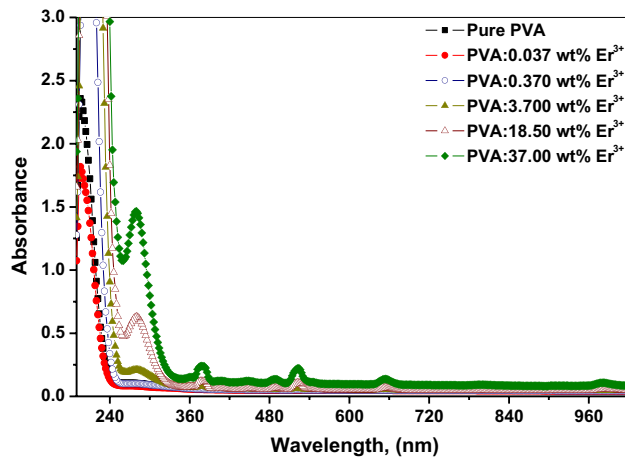


Fig. 5 UV-vis-NIR absorbance of pure PVA and various wt% Er³⁺-doped PVA polymeric samples

reported previously for a polymeric material with rare earth ions [15]. This indicates the increase in the random order within the base samples by the complexes formed between the RE ions and cations of the fundamental chain. In the absorption spectra (Fig. 5), some ripples in the pure PVA, at 281, 377, 520, 655 and 981 nm, increased with increasing the Er³⁺-ion concentrations. Moreover, there is a very slight shift of the peak at 281 nm towards higher wavelength of 285 nm for 37 wt% of Er³⁺-ion that is explained by the H- bonding between Er³⁺-ions and the matrix of PVA. This peak refers to *n*– π^* electronic transition of the (C=O) carbonyl groups in PVA [16]. Also, the optical absorption of

the polymeric films increased with further content level of Er³⁺-ions within PVA, similar to that reported for Ce³⁺, Gd³⁺, Sm³⁺ and Eu³⁺ in PVA polymer films [23, 24]. Moreover, with raising the doping level of Er³⁺-ions in PVA matrix, the light was fully absorbed/blocked in the UV-region band. Therefore, PVA: 37 wt% Er³⁺-sample can be used as an excellent UV-protector.

Furthermore, the direct, E'_g , and indirect, E_g , energy gap of the non-crystalline materials were calculated using the following relations [25]:

$$\alpha = 2.303 \frac{B}{X(\text{cm})} \tag{4}$$

$$(\alpha h\nu)^{1/m} = B(h\nu - E_g^{\text{Opt}})^m, \tag{5}$$

where B and α are the energy constant (absorbance), and the absorption coefficient. As the values of the direct, $m = 1/2$, and indirect, $m = 2$, allowed transitions are determined by extrapolating a line to zero absorption in the plotting of $(\alpha h\nu)^{1/m}$, with $(h\nu)$, as presented in Figs. 6 and 7. All the values of the energy gap are recorded in Table 1. The E'_g , and E_{g1} values are equal to 5.6 eV and 4.98 eV for the base sample, whereas for PVA:37 wt% Er³⁺-ions film they were 5.08 eV and 4.74 eV, respectively. This decrease in the band gap with further Er³⁺-ions content was observed in previous work of filler-doped PVA [2, 26]. However, this proved the formation of energy levels which are created in the mobility gap of Er³⁺/ PVA films, which facilitated the crossing of electrons. This result is related to the influence of the

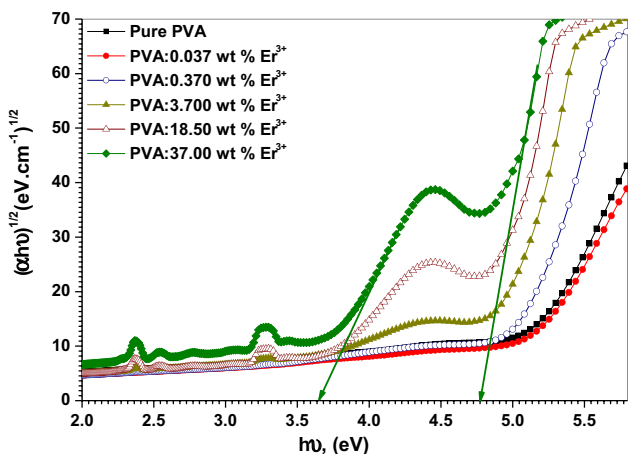
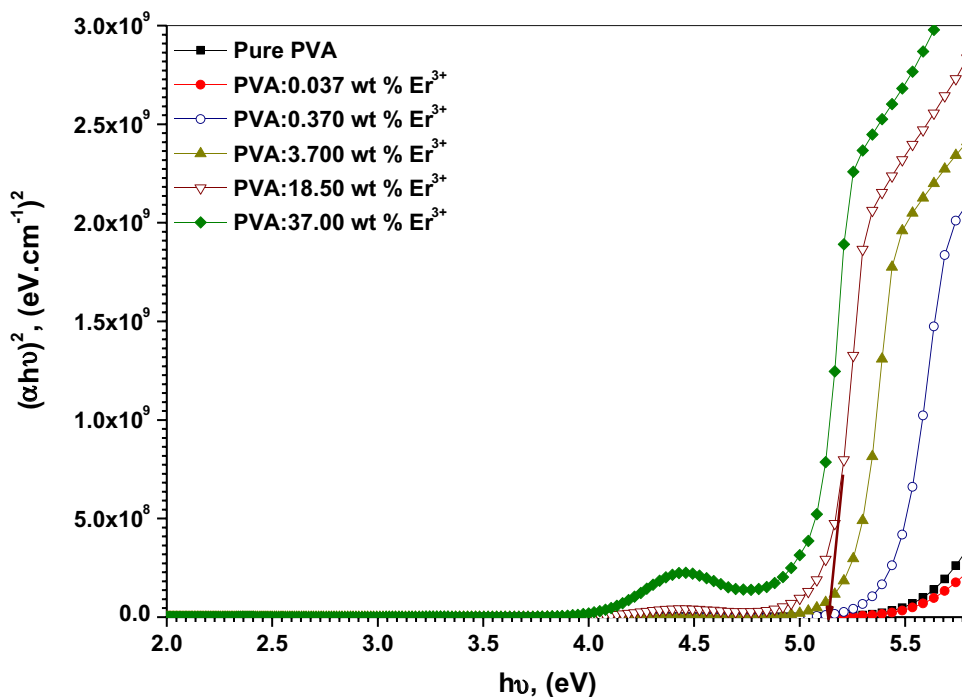


Fig. 6 The variation of $(\alpha h\nu)^{1/2}$ with energy of applied photon for pure PVA and various wt% Er³⁺-doped PVA polymeric samples

Fig. 7 The variation of $(\alpha h\nu)^2$ with energy of applied photon for pure PVA and various wt% Er³⁺-doped PVA polymeric samples



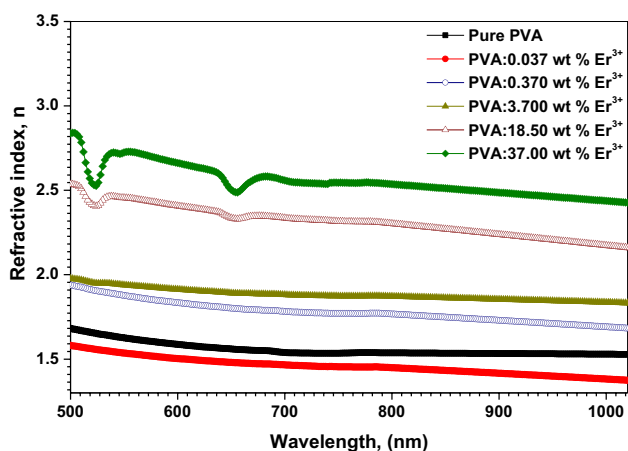


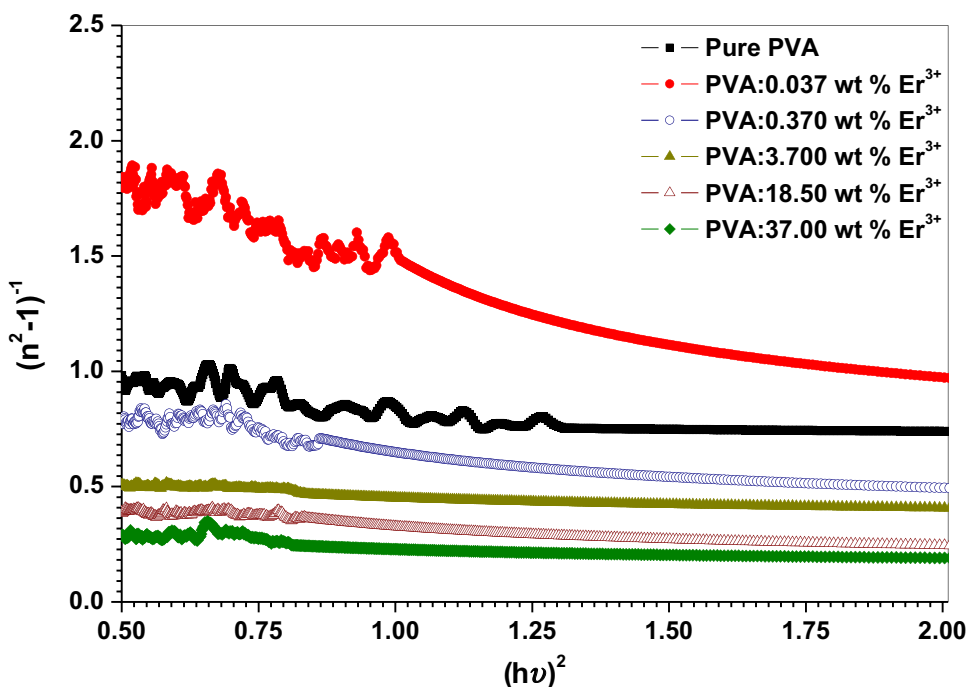
Fig. 8 Variation of the refractive index (n) with the wavelength (λ) of the incident photon for pure PVA and various wt% Er^{3+} -doped PVA polymeric samples

complex bonding of Er^{3+} -ions with O–H of PVA chains. Similarly, the effect on the energy band gap is reported in other work [1, 15].

One of the power parameters in optical physics is the index of refraction, n , which is more significant for designing optical communication and spectral dispersion devices. The following formula was used to calculate the n values [27]:

$$n = \frac{(1 + R)}{(1 - R)} + \sqrt{\frac{4R}{(1 - R)^2} - k^2}, \tag{6}$$

Fig. 9 Variation of $(n^2 - 1)^{-1}$ with $(h\nu)^2$ for of pure PVA and various wt% Er^{3+} -doped PVA polymeric samples



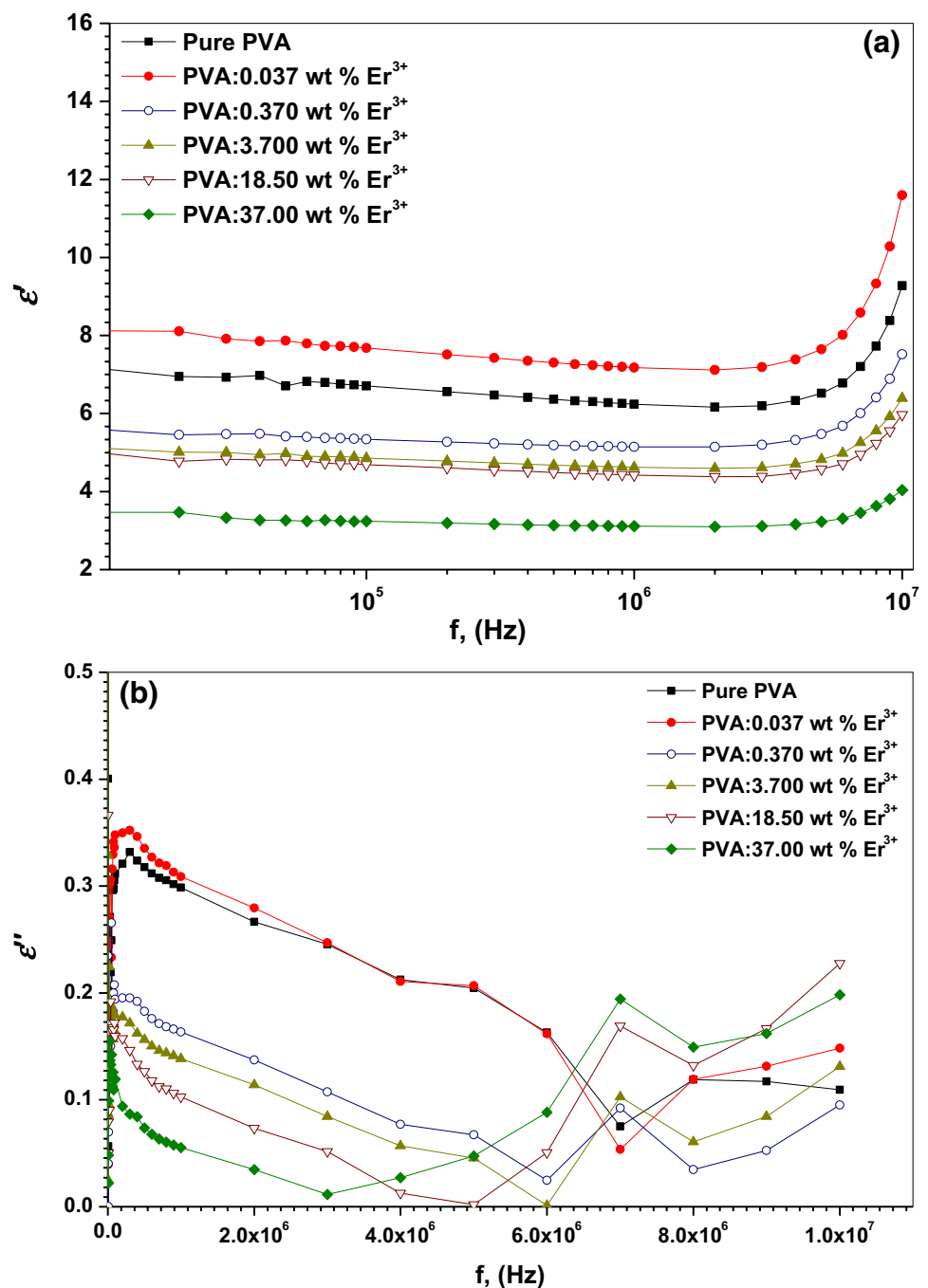
where R and k are called the reflectance and the extinction index. The base sample has n values between 1.53 and 1.67 in the range of 2000–950 nm, while the maximum value lies between 2.44 and 2.84 for PVA: 37 wt% Er^{3+} -ions sample in the same range (Fig. 8). However, these values are more than that reported for PVA with ErCl_3 [28] and La^{3+} -doped PVA samples [2]. Moreover, it is clear that n value increased with the increase of Er^{3+} -ions contents in the PVA. The results are comparable to previous work reported on PVA: ErCl_3 [28]. The n value of the material depends on the internal structure like the packing density and molecular weight distributions factors. Therefore, the highest electronegative ions like Er^{3+} -ions (1.24 eV) increase the degree of the disorder in the matrix of PVA by forming ion- legend complexes inside the polymer that arise more mobilities of the free radicals and increase the value of n [29].

The single dispersion energies (E_d) and the average oscillator energy for electronic transitions (E_s) in the Er^{3+} /PVA films were calculated by plotting the relation between $(n^2 - 1)^{-1}$ and $(h\nu)^2$ with the help of the single effective oscillator model [30]:

$$\frac{1}{n^2 - 1} = \frac{E_s}{E_d} - \frac{(h\nu)^2}{E_d E_s} \tag{7}$$

Therefore, in Fig. 9, the slope of the linear part and the intercept values with the y-axis of that relation were used to determine E_d and E_s for all films. As recorded in Table 1, the E_d value increased, whereas the E_s decreased with an increment of Er^{3+} -ions content within PVA. These show the

Fig. 10 The dielectric permittivity ϵ' (a) and dielectric loss ϵ'' (b) versus frequency for pure PVA and all prepared Er^{3+} -doped PVA polymeric samples



strong effect of the addition of Er^{3+} -ions in the base sample. These results are similar to the other work reported on La^{3+} -doped PVA and PVA– Al_2O_3 composite films.

3.5 Dielectric analyses of Er^{3+} /PVA composite films

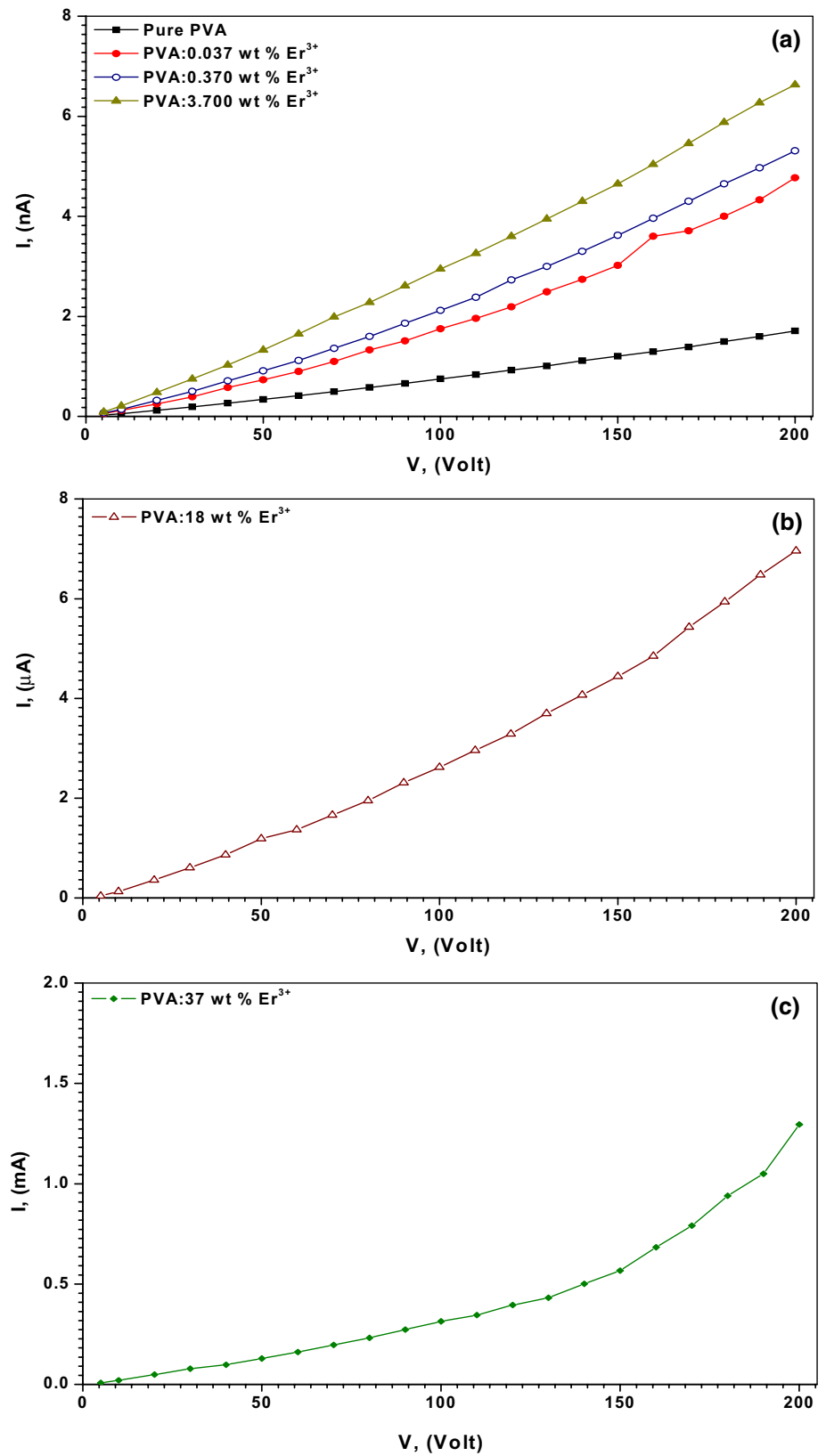
The permittivity ϵ' , and the loss ϵ'' of the dielectric Er^{3+} /PVA samples are expressed, respectively, by the following relations [31]:

$$\epsilon' = \frac{C(F).X(m)}{\epsilon_o(F.m^{-1}).A(m^2)}, \tag{8}$$

$$\epsilon'' = \epsilon' . \tan \delta, \tag{9}$$

where C is the capacitance of the sample. Figure 10(a, b) show the variation of the dielectric permittivity, ϵ' , and loss, ϵ'' , with different ratios of Er^{3+} -ions, in air, over the range 3 kHz–10 MHz. It was reported that ϵ' does not depend only on the different frequencies, but also the ratio of the doping

Fig. 11 Variation of current- voltage characteristics of pure PVA, PVA:0.037 wt% Er^{3+} , PVA:0.37 wt% Er^{3+} , and PVA:3.7 wt% Er^{3+} (a), PVA: 18 wt% Er^{3+} (b), and PVA: 37 wt% Er^{3+} (c) films



in polymeric composite films [4]. As presented in Fig. 10a, the ϵ' values decreased by increasing the wt% of Er^{3+} -ions compared to the base polymer, which can be explained by the effect of the complex interaction between the reacting substances, as well as, the conductivity effects that cause a decrease of polarization via the increment of the charge carriers of the continuous network inside the composite films. Figure 10b shows that the base polymeric sample, at low frequencies, has a higher value of dielectric loss compared to the others. However, at higher frequencies, the losses of samples, with high Er^{3+} -ions content, increased which can be due to the vibration of molecules in the crystalline region of the PVA main chain.

3.6 I – V characteristic curve of Er^{3+} /PVA composite films

The effect of variable concentration of Er^{3+} -ions on I – V characteristic of PVA is illustrated in Fig. 11a–c. It was observed that as the applied potential difference increases, the associated electric current values increase. Also, the values of the current increase with the Er^{3+} -ion content. However, another trend has been noticed in the case of zero and low content of Er^{3+} -ions in PVA matrix; the I – V characteristics are linear, and the samples have an Ohmic behavior. It can be noticed that with high doping of erbium nitrate (18 wt% and 37 wt%), the nonlinear behaviors of the I – V characteristics were induced at the high applied voltage. This could be related to two reasons: the first one is the decreasing of the resistance of the sample and the other one is due to further addition of Er^{3+} -ions that establish a new level inside the gap of the base sample [4, 32]. Thereby at high voltage, the narrow region in the band gap permits more charges to jump between levels, which associated with the increase in the electric current values from nA to mA. However, the current values for PVA: 18.5 wt% Er^{3+} and PVA: 37 wt% Er^{3+} are larger than that reported for PVA doped La^{3+} -ions [2]. So, a new and cheaper varistor device can be made by the preparation of polymeric samples with a high content of rare earth-like Er^{3+} -ion.

4 Conclusions

A successful synthesis of PVA films with different concentrations of Er^{3+} is achieved at low temperature through a low-cost technique. The structure between amorphous and crystalline is observed by XRD, whereas the production of Er^{3+} /PVA complex is confirmed by FTIR. Moreover, the agglomeration of Er^{3+} -ion increase, and a larger cluster size is formed on the superficiality of PVA:37 wt% Er^{3+} -sample approved by SEM. The dielectric, the electrical and the

optical properties vary with the percentage of Er^{3+} -doping. Due to the absorption property of PVA: 37 wt% Er^{3+} -sample within the UV–vis region, this film can be used as a promising material for excellent UV-protector. The E'_g , and E_g values are found to be 5.08 eV and 4.74 eV for PVA: 37 wt% Er^{3+} -film. The n values for pure PVA are observed between 1.37 and 1.53, while for PVA:37 wt% Er^{3+} , between 1.98 and 2.46 in range of 2000–950 nm. Therefore, these samples are promising materials to utilize in optoelectronic applications. The electrical characterization of the as-prepared films presents a non-linear I – V behavior and the electrical current value changed from nA to mA by increasing wt% of Er^{3+} -ions, which are significant factors for new varistor devices that work at high voltage.

Acknowledgements The authors extend their appreciation to the Deanship of Scientific Research at King Khalid University for funding this work through research groups program under Grant Number R.G.P.1/59/39.

References

1. B. Adhikari, S. Majumdar, Prog. Poly. Sci. **29**, 699–766 (2004)
2. H. Elhosiny Ali, Y. Khairy, H. Algarni, H.I. Elsaedy, A.M. Alshehri, I.S. Yahia, J. Mater. Sci. Mater. Electron. **29**, 20424–20432 (2018)
3. M.N. Muralidharan, S. Mathew, A. Seema, P. Radhakrishnan, T. Kurian, Mater. Chem. Phys. **171**, 367–373 (2016)
4. Q. Li, T. Li, J. Wu, J. Phys. Chem. B. **105**, 12293–12296 (2001)
5. M.A.F. Basha, Polym. J. **42**, 728–734 (2010)
6. M.O. Reddy, B.C. Babu, Ind. J. Mater. Sci. **8**, 927364 (2015)
7. S. DÖkme, I. Altindal, Uslu, J. Appl. Polym. Sci. **125**(2), 1185 (2012)
8. C.V. Subba Reddy, X. Han, Q.Y. Zhu, L.-Q. Mai, W. Chen, Microelectron. Eng. **83**, 281 (2006)
9. T.A. Hanafy, J. Appl. Phys. **112**, 034102 (2012)
10. Y. Chen, S. Zhou, F. Li, F. Li, Y. Chen, J. Lumin **131**, 701–704 (2011)
11. M.M. Lezhnina, U.H. Kynast, Opt. Mater. **33**, 4–13 (2010)
12. R.F. Bhajantri, V. Ravindrachary, A. Harisha, C. Ranganathaiah, G.N. Kumaraswamy, Appl. Phys. A Mater. Sci. Process. **87**, 797–805 (2007)
13. L. Ke, M. Hu, X. Ma, J. Matt. **726314**, 5 (2013)
14. L.-M. Zhao, X. Shao, Y.-B. Yin, W.-Z. Li, Mater. Res. Bull. **44**, 1334–1338 (2009)
15. J.K. Rao, A. Raizada, D. Ganguly, M.M. Nankad, S.V. Satyanarayana, G.M. Madhu, J. Mater. Sci. **50**, 7064–7074 (2015)
16. R.P. Chahal, S. Mahendia, A.K. Tomar, S. Kumar, J. Alloy. Compd. **538**, 212–219 (2012)
17. L. Alexander, H.P. Klug, J. Appl. Phys. **21**, 137–142 (1950)
18. A.M. Mefteh, E. Gharibshahi, N. Soltani, W.M.M. Yunus, E. Saion, Polymers **6**, 2435–2450 (2014)
19. R.P. Chahal, S. Mahendia, A.K. Tomar, S. Kumar, J. Opt. Mater. **52**, 237–241 (2016)
20. R.P. Chahal, S. Mahendia, A.K. Tomar, S. Kumar, Appl. Surf. Sci. **343**, 160–165 (2015)

21. J.K. Rao, A. Raizada, D. Ganguly, M.M. Mankad, S.V. Satayanarayana, G.M. Madhu, *J. Mater. Sci.* **50**, 7064–7074 (2015)
22. S. More, R. Dhokne, S. Moharil, *Polym. Bull.* **75**, 909–923 (2018)
23. B. Karthikeyan, *Chem. Phys. Lett.* **432**, 513–517 (2006)
24. K.H. Mahmoud, Z.M. El Bahy, A.I. Hanafy, *J. Phys. Chem. Solid.* **72**, 1057–1065 (2011)
25. K.S. Hemalatha, K. Rukmani, N. Suriyamurthy, B.M. Nagabhushana, *Mater. Res. Bull.* **51**, 438–446 (2014)
26. I.S. Yahia, S.M. Keshk, *Opt. Laser Technol.* **90**, 197–200 (2017)
27. A.M. El Sayed, W.M. Morsi, *J. Mater. Sci.* **49**, 5378–5387 (2014)
28. T.A. Hamdalla, T.A. Hanafy, A.E. Bekheet, *J. Spect.* **204867**, 7 (2015)
29. S. Xu, Z. Yang, S. Dai, J. Yang, L. Hu, Z. Jiang, *J. Alloys Compd.* **361**, 313–319 (2003)
30. N.M. Shah, J.R. Ray, K.J. Patel, V.A. Kheraj, M.S. Desai, C.J. Panchal, B. Rehani, *Thin Solid Films* **517**, 3639–3644 (2009)
31. A. Tataroglu, S. Altındal, M.M. Bulbul, *Microelectron. Eng.* **81**, 140–149 (2005)
32. A.M. El Sayed, S. El-Gamal, W.M. Morsi, Gh. Mohammed, *J. Mater. Sci.* **50**, 4717–4728 (2015)